

## Efficient, Indirect Transverse Laser Cooling of a Fast Stored Ion Beam

H.-J. Miesner, R. Grimm, M. Grieser, D. Habs,\* D. Schwalm, B. Wanner,<sup>†</sup> and A. Wolf

Max-Planck-Institut für Kernphysik and Physikalisches Institut der Universität Heidelberg, D-69029 Heidelberg, Germany

(Received 28 November 1995)

Three-dimensional laser cooling of a fast stored ion beam has been demonstrated at the Heidelberg Test Storage Ring. With a purely longitudinal cooling force applied to a 7.3 MeV  ${}^9\text{Be}^+$  beam, we have observed an efficient transverse cooling effect. We interpret this observation as being due to a thermal intrabeam relaxation between the different degrees of freedom that is caused by Coulomb collisions of the stored particles. [S0031-9007(96)00673-4]

PACS numbers: 32.80.Pj, 29.20.Dh, 42.50.Vk

The success of storage-ring experiments with charged particle beams often relies on the application of cooling methods [1]. Laser cooling, as applicable to a selected number of heavy-ion species, is by far the most efficient longitudinal cooling technique [2–5] and offers unique possibilities for studying the beam dynamics at very high phase-space densities, where a variety of new phenomena is expected to occur up to a possible crystallization of the beam [6,7].

A direct transverse laser cooling of fast stored ion beams, which has not been demonstrated yet, appears to be very difficult, because the interaction times are very short, and first-order Doppler shifts make the optical resonance extremely sensitive to angular misalignments between laser and ion beam. The existence of a transverse-longitudinal relaxation [8] or coupling mechanism [9], however, can facilitate an efficient three-dimensional cooling, even with purely longitudinal laser cooling. In this Letter, we report the first experimental demonstration of such an indirect transverse laser cooling.

In our experiments performed at the Heidelberg Test Storage Ring (TSR), typically  $3 \times 10^7$   ${}^9\text{Be}^+$  ions are injected at an energy of 7.3 MeV, which corresponds to an ion current of  $1 \mu\text{A}$ . At a ring vacuum of  $3 \times 10^{-11}$  mbar rest-gas collisions limit the  $1/e$  storage lifetime to 25 s. Standard electron cooling is applied to precool the ion beam [10] and reduces the ion beam diameter from 2 cm after injection to  $\sim 1$  mm.

The laser beam is merged with the ion beam in one of the straight sections of the storage ring over a length of  $\sim 5$  m. The laser frequency is nearly resonant with the  $D_2$  transition of the alkali-like  ${}^9\text{Be}^+$  ion ( $1s^2 2s^2 S_{1/2} \rightarrow 1s^2 2p^2 P_{3/2}$ ), which has a rest-frame wavelength of 313.13 nm. In the laboratory frame this wavelength is Doppler shifted to 300.35 nm at the chosen ion beam velocity of 4.17% of the speed of light for copropagating beams. This particular choice of the velocity allows us to use fixed-frequency argon-ion lasers.

The hyperfine-split transition can be modeled as a  $\Lambda$ -type scheme, as the ground state splitting between the  $F = 1$  and  $F = 2$  state amounts to 1.25 GHz while the splitting of the excited states is negligibly small compared

to the natural linewidth of 19.3 MHz. To obtain a closed excitation scheme we use two laser fields, produced by two separate argon-ion lasers (Coherent Innova 400), with the corresponding difference frequency of 1.30 GHz in the laboratory frame. The frequency of one laser is locked to an optical cavity which itself is locked to a long term frequency-stable He-Ne laser. For locking the frequency of the second laser 1.30 GHz apart we use the optical beat signal of the two laser fields. The intensity of the laser beam was  $2 \times 20$  mW, resulting in an effective on-resonance saturation parameter of up to  $S \approx 20$  at the beam waist of 0.7 mm in the center of the laser-cooling section.

The longitudinal laser-cooling force that we apply to the stored ion beam is shown in Fig. 1. It consists of three different contributions: (i) The narrow resonance peak centered at the velocity  $v_0$  is the usual resonant light-pressure force exerted by the laser [4]. Because of the Doppler

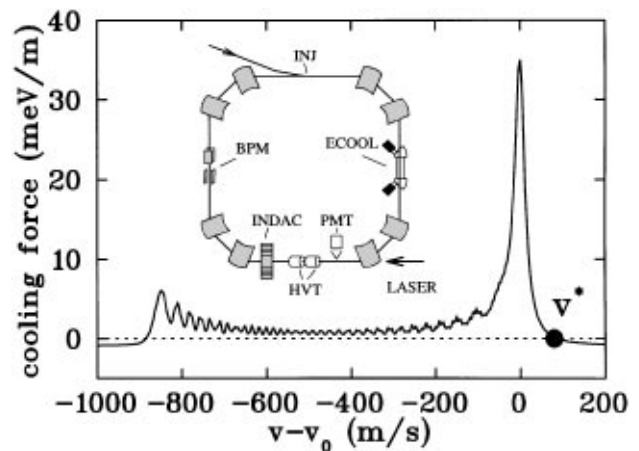


FIG. 1. Longitudinal, ring-averaged cooling force, as calculated for the experimental parameters. The resonant ion velocity  $v_0$  is about  $1.25 \times 10^7$  m/s, and the ions are kept at the stable point  $v^*$ . The inset shows a schematic view of the TSR with its circumference of 55.4 m: INJ, injection; ECOOL, electron cooler; PMT, photomultiplier tube; HVT, high-voltage biased drift tubes; INDAC, induction accelerator; BPM, beam profile monitor; not shown are the 20 quadrupole magnets of the focusing structure.

effect it reflects the Lorentzian excitation line shape as a function of the ion velocity. (ii) The broad structure extending from the resonant velocity  $v_0$  down to about  $v_0 - 900$  m/s is due to a special capture range extension of the light-pressure force, as explained below. (iii) The accelerating laser force is counteracted by a velocity-independent, decelerating auxiliary force generated with the help of an induction accelerator [4]. This is necessary to create a stable cooling point (see dot in Fig. 1), in the vicinity of which the combined force  $F(v)$  can be approximated as a simple friction force  $F(v) \approx -\alpha(v - v^*)$ . From the friction coefficient  $\alpha$  the longitudinal laser-cooling rate can be calculated as  $\Lambda_{\parallel} = 2\alpha/m$ , where  $m$  is the ion mass. In the experiments, we applied a counteracting force of  $-0.9$  meV/m and obtained a longitudinal cooling rate of  $\Lambda_{\parallel} = 100 \pm 50$  s $^{-1}$ ; the linear approximation to the cooling force holds in a velocity interval of a few 10 m/s, i.e., for temperatures of up to a few kelvin.

The extension of the capture range of the cooling force to its low-velocity side eliminates a severe loss of laser-cooled ions, which otherwise occurs as a result of close binary Coulomb collisions in the transversely hot beam. These collisions can transfer a considerable amount of the transverse kinetic energy of an ion into its longitudinal motion [4,11]. In the electron-precooled  ${}^9\text{Be}^+$  beam, this can lead to abrupt longitudinal velocity changes of up to  $\sim 1000$  m/s. The capture range extension is realized in a simple way with the help of an arrangement of drift tubes, which is located in the laser-cooling section of the TSR and is biased to negative voltages of the order of  $-1$  kV. The basic idea of this method [12] is that the ions are locally accelerated in the fringe fields of the tubes, so that the Doppler shift results in frequency chirps as “seen” by the ions. These chirps force the ions to absorb photons in so-called adiabatic passages and, under our experimental conditions, accelerate them back to the stable point with a ring-averaged force of at least 2 meV/m. Details of this method will be given elsewhere.

For diagnostics, the longitudinal velocity distribution of the ions collected at the stable cooling point is probed in a standard way [4] by ramping the bias voltage of a simple drift tube installed in the laser-cooling section and detecting the intensity of the fluorescence light that is induced by the cooling laser itself inside the drift tube. The ring-averaged transverse temperatures  $T_h$  and  $T_v$  in the horizontal and vertical directions, respectively, are derived from the corresponding Gaussian-shaped beam profiles, measured at the location of the beam profile monitor [13]. This device is based on the position sensitive detection of residual gas ions originating from collisions with the ion beam. Following Ref. [4], we obtain the numerical relations  $T_h = (50\,000\text{ K})(\sigma_h/\text{mm})^2$  for the horizontal and  $T_v = (34\,000\text{ K})(\sigma_v/\text{mm})^2$  for the vertical directions, where  $\sigma_h$  and  $\sigma_v$  denote the standard deviations for the horizontal and vertical position spreads, respectively [14]. As a consequence of the limited knowledge of the

TSR lattice functions, we estimate systematic uncertainties in the proportionality factors of about  $\pm 10\%$ . The resolution  $\sigma_{\text{res}} = 0.19 \pm 0.02$  mm of the beam profile monitor is quadratically subtracted from the measured data, since both the resolution function and the measured profiles are to a very good approximation found to be of Gaussian shape. This means that we subtract horizontal and vertical resolution temperatures of 1800 and 1200 K with uncertainties of 400 and 250 K, respectively.

A set of measurements demonstrating the three-dimensional beam cooling is displayed in Fig. 2, where the temporal evolution of the beam temperatures starts with the beam injection at  $t = 0$  s. After 5 s of electron precooling the ion beam reaches transverse equilibrium temperatures of  $T_h = 4000$  K and  $T_v = 500$  K. Then, without any further cooling applied, the beam heats up in all degrees of freedom. At higher temperatures this typical “blowup” behavior significantly slows down with decreasing beam density. When laser cooling starts, the measured longitudinal temperature  $T_{\parallel}$  decreases rapidly to a value of  $\sim 6$  K. Instantly, the transverse degrees of freedom begin to cool down and nearly reach equilibrium [15] within the time of longitudinal cooling, which is technically limited to 5 s by the maximum ramping time of the induction accelerator. During the transverse cooling process,  $T_{\parallel}$  increases and slowly approaches  $\sim 15$  K.

For an interpretation of these observations it is useful to consider the energy flow diagram shown in Fig. 3. The high kinetic energy serves as a large reservoir, from which energy is permanently transferred into the thermal

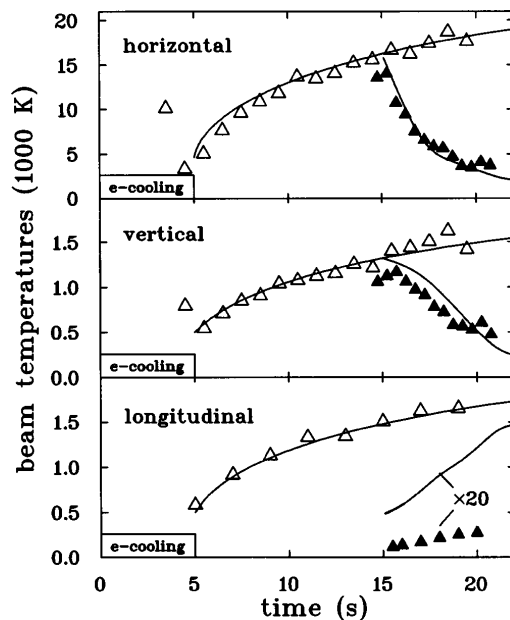


FIG. 2. Temporal evolution of the beam temperatures, observed without any further cooling after electron precooling (open symbols) and with laser cooling applied after 10 s (solid symbols). The solid lines show corresponding numerical results obtained from IBS theory (see text).

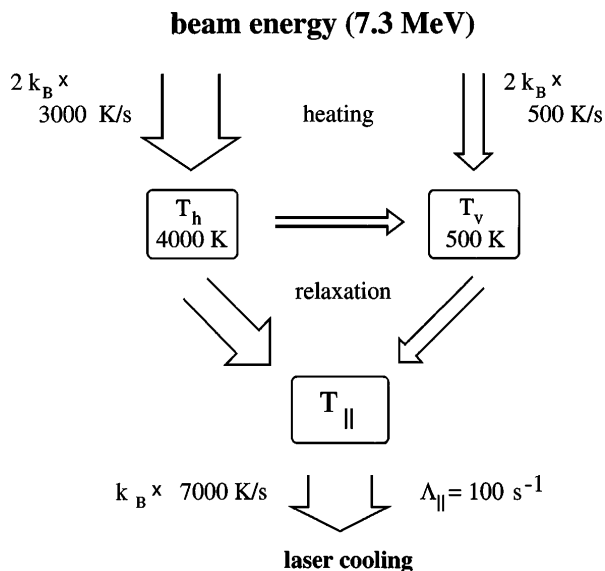


FIG. 3. Equilibrium energy-flow diagram for the stored ion beam with longitudinal laser cooling.

transverse motion. This beam heating results from intra-beam Coulomb scattering in the bending and alternating-gradient focusing structure of the storage ring [16,17]. The resulting growth of the horizontal temperature in an uncooled beam is much more pronounced than the vertical one, because the horizontal degree of freedom shows larger variations of the focusing strength, and also because of the dependence of the closed orbit on the longitudinal velocity, i.e., the storage-ring dispersion, which amounts to 1.2 m in an average over the TSR lattice.

In addition to this external heating, the intrabeam scattering (IBS) causes a *thermal relaxation between all degrees of freedom*. If a cooling mechanism is applied, even only in one dimension, this intrabeam relaxation tends to establish an equilibrium between heating and cooling in all three degrees of freedom. When laser cooling starts in the transversely hot beam, it first reduces the longitudinal temperature and thus brings the beam into pronounced nonequilibrium. Then, on the much longer time scale of a few seconds, the subsequent equilibration leads to the indirect transverse cooling, as demonstrated by the experimental data in Fig. 2. During this process the phase-space density increases, which results in a stronger beam heating and which qualitatively explains the observed increase of the measured values of  $T_{||}$ .

For the equilibrium under our experimental conditions, we find a beam heating associated with the energy transfer per particle and time from the kinetic beam energy into the potential and kinetic energy of the transverse betatron oscillations of horizontally  $2k_B(3000 \pm 1000 \text{ K/s})$  and vertically  $2k_B(500 \pm 250 \text{ K/s})$ . The given values are derived from additional beam blowup measurements, performed right after switching off the laser cooling. In the equilibrium balance of heating and cooling, it then follows

that the laser cooling dissipates  $k_B(7000 \pm 2500 \text{ K/s})$  out of the longitudinal motion.

Only a part of this dissipation rate can be explained by the measured longitudinal temperatures of the ions in the vicinity of the stable point: Together with the cooling rate  $\Lambda_{||} = 100 \pm 50 \text{ s}^{-1}$ , the equilibrium temperature  $T_{||} = 15_{-2}^{+5} \text{ K}$  gives a dissipation rate of  $\Lambda_{||}T_{||} = 1500_{-850}^{+1500} \text{ K/s}$ . We believe that the remaining part of energy dissipation is due to a second, unobserved component in the longitudinal velocity distribution, which is much broader than the linear range of the cooling force and which could not be discriminated against the noise in our probe scans. This “hot” subdistribution [18], containing only a small fraction of all ions, is formed by those particles which, after large longitudinal velocity changes in rare close collisions [11], are driven back to the stable point.

Let us compare the results to a calculation based on “standard” IBS theory. We use the computer code INTRABS [19], which incorporates the analytical model of [20] and calculates the rms velocity changes for all degrees of freedom under the simplifying assumption of Gaussian velocity distributions. With the specific lattice functions of the TSR, the ion mass and charge, storage lifetime, initial number and temperatures of the ions, and the longitudinal cooling rate as input data, the program calculates the temporal evolution of the beam temperatures [21]. For the  ${}^9\text{Be}^+$  beam, the solid lines in Fig. 2 show the corresponding results, which very well reproduce the beam blowup for an injected ion number of  $2 \times 10^7$ . The temporal evolution of the laser-cooling process is calculated with the cooling rate  $\Lambda_{||} = 100 \text{ s}^{-1}$ . The resulting longitudinal temperatures are clearly higher than the measured ones, which again points to the fact that we have only observed a cold component of a bimodal longitudinal velocity distribution, where the unobserved hot subdistribution mentioned above gives a substantial contribution to the rms velocity spread. This, however, seems to have no significant influence on the indirect transverse cooling, which appears to be well described.

In a further series of experiments, we have studied the dependence of the indirect transverse cooling process on the initial temperatures simply by varying the time delay between laser cooling and electron precooling. In Fig. 4 we show the combined results of four sets of corresponding measurements together with a blowup over the full time. The transverse cooling does not critically depend on the delay that sets the initial conditions, i.e., the increasing initial temperatures and the number of ions as decreasing with the storage lifetime of  $\sim 25 \text{ s}$ . When laser cooling is applied, the transverse temperatures reach equilibrium within at least 4 s. From these measurements one derives for both transverse degrees of freedom an indirect cooling rate of  $\Lambda_{\perp} \approx 1 \text{ s}^{-1}$ , which is consistent with the observed equilibrium temperatures in a balance between transverse heating and cooling (see also Fig. 3). Even for rather low longitudinal laser-cooling rates in these experiments, the

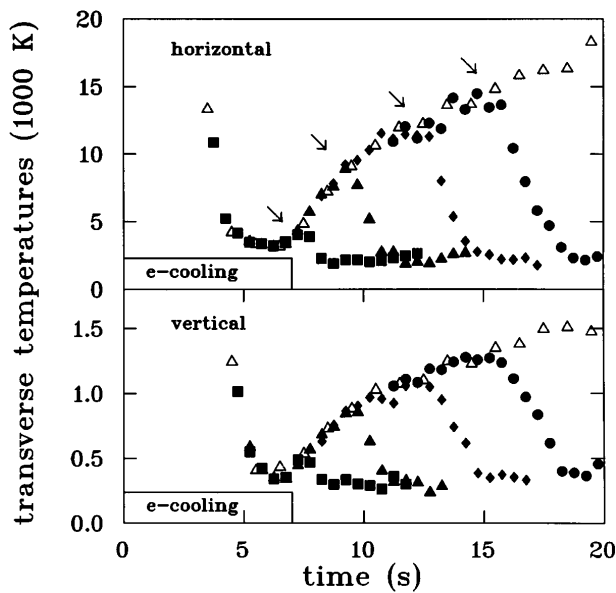


FIG. 4. Temporal evolution of the transverse beam temperatures, observed for laser cooling with various delays after electron precooling. The arrows mark the respective beginning of the laser-cooling process.

results already show transverse equilibrium temperatures below those of the electron-cooled ion beam.

Standard IBS theory predicts  $\Lambda_{\perp}$  to scale linearly with the longitudinal cooling rate  $\Lambda_{\parallel}$ , and the equilibrium temperatures in all degrees of freedom are predicted to scale as  $\Lambda_{\parallel}^{-0.42}$ , with an exponent weakly depending on the specific ring lattice. With a thousandfold increase of  $\Lambda_{\parallel}$ , which is in principle offered by laser cooling, we may therefore expect a possible  $\Lambda_{\perp}$  of the order of  $1000 \text{ s}^{-1}$  along with temperatures 20 times lower than the already demonstrated ones; this would also mean a 20 times higher number density of the beam. Conditions close to this optimum scenario seem to be attainable with radio-frequency bunched ion beams [5], where maximum longitudinal cooling rates can be applied without the problem of collisional losses. With this scheme, improved experiments on the indirect transverse cooling are in progress at the TSR.

We thank D. Möhl for valuable discussions on intra-beam scattering. This work was supported in part by the Bundesministerium für Forschung und Technologie under Contract No. 06HD525I.

\*Now at Ludwig-Maximilians-Universität München, Am Coulombwall 1, D-85748 Garching, Germany.

†Present address: Institut d'Optique Théorique et Appliquée, 91403 Orsay, France.

- [1] *Proceedings of the Workshop on Beam Cooling and Related Topics, Montreux, Switzerland, 1993*, edited by J. Bosser (CERN Report No. 94-03, 1994).
- [2] S. Schröder *et al.*, Phys. Rev. Lett. **64**, 2901 (1990).
- [3] J. S. Hangst *et al.*, Phys. Rev. Lett. **67**, 1238 (1991).
- [4] W. Petrich *et al.*, Phys. Rev. A **48**, 2127 (1993).
- [5] J. S. Hangst *et al.*, Phys. Rev. Lett. **74**, 4432 (1995).
- [6] A. Rahman and J. P. Schiffer, Phys. Rev. Lett. **57**, 1133 (1986).
- [7] D. Habs and R. Grimm, Annu. Rev. Nucl. Part. Sci. **45**, 391 (1995), and references therein.
- [8] H.-J. Miesner *et al.*, *Fourteenth International Conference on Atomic Physics (ICAP-14), Boulder, 1994, Book of Abstracts* (American Institute of Physics, New York, 1994), p. 1L-2.
- [9] H. Okamoto, A. M. Sessler, and D. Möhl, Phys. Rev. Lett. **72**, 3977 (1994).
- [10] S. Pastuszka *et al.*, Nucl. Instrum. Methods Phys. Res., Sect. A **369**, 11 (1996).
- [11] H.-J. Miesner *et al.*, in Ref. [1], p. 349.
- [12] B. Wanner *et al.*, in Ref. [1], p. 354.
- [13] B. Hochadel *et al.*, Nucl. Instrum. Methods Phys. Res., Sect. A **343**, 401 (1994).
- [14] The beam emittances are proportional to the ring-averaged temperatures. For the TSR lattice we obtain  $T_h = 2.2 \times 10^{10} \epsilon_h \text{ K}/(\pi \text{ m rad})$  and  $T_v = 1.1 \times 10^{10} \epsilon_v \text{ K}/(\pi \text{ m rad})$ .
- [15] Our statement that we have almost reached equilibrium is confirmed by similar experiments with shorter time delays between electron precooling and laser cooling. In this case, the total equilibration time is much shorter and the steady state is clearly visible; see also Fig. 4.
- [16] A. H. Sørensen, in *Proceedings of the CERN Accelerator School*, edited by S. Turner (CERN Report No. 87-10, 1987).
- [17] M. Seurer *et al.*, Nucl. Instrum. Methods Phys. Res., Sect. A **351**, 286 (1994).
- [18] T. O. Raubenheimer, Part. Accel. **45**, 111 (1994).
- [19] R. Giannini and D. Möhl (private communication).
- [20] A. Piwinski, in *Proceedings of the 9th International Conference on High Energy Accelerators, Stanford, 1974*; M. Martini, CERN Report No. PS/84-9 (AA), 1984; A. Piwinski, in *Proceedings of the CERN Accelerator School*, edited by S. Turner (CERN Report No. 87-03, 1987).
- [21] Detailed measurements on the blowup of electron-precooled beams performed for a broad variety of beam energies and charge states have shown that in the case of the standard TSR lattice the vertical blowup rate is always calculated to be a factor of 8.3 higher than it is experimentally observed; see B. Hochadel, Max-Planck-Institut für Kernphysik Report No. MPIH-V34-1994. Therefore, in order to describe the TSR data, we modified the original program and artificially reduced the vertical heating rate by the above-mentioned factor.